Supporting Information

Enhanced UV-light Stability of Planar Heterojunction Perovskite Solar Cells Based on CsBr modification

Wenzhe Li,†[a,b] Wei Zhang,†[a] Stephan Van Reenen,[a] Rebecca J. Sutton,[a] Jiandong Fan,[a] Amir A. Haghighirad,[a] Michael B. Johnston,[a] Liduo Wang,[b] and Henry J. Snaith*[a]*

† These authors contribute equally to the work.
Clarendon Laboratory, University of Oxford, Parks Road, Oxford OX1 3PU, UK
E-mail: h.snaith1@physics.ox.ac.uk
Department of Chemistry, Tsinghua University, Beijing 100084, China
E-mail: chldwang@mail.tsinghua.edu.cn.

Experimental Section

Substrate Preparation: Devices were fabricated on fluorine-doped tin oxide (FTO) coated glass (Pilkington, 7Ω·cm^{-1}). Initially FTO was etched with 2 mol/L HCl and zinc powder. Substrates were then cleaned sequentially in 2% Hellmanex^{TM} detergent, deionized water, acetone, isopropanol and oxygen plasma. A hole-blocking layer of compact TiO_2 was deposited by spin-coating a mildly acidic solution of titanium isopropoxide in ethanol (the concentrations of titanium isopropoxide/2M HCl/ethanol=254μL/34μL/2mL) at 2000 rpm for 60 s, which was then annealed in air at 500 °C for 30 min.

CsBr interface modification: The CsBr modification layer was prepared by spin-coating a solution of 2.5 mg/ml (unless otherwise stated) CsBr (Sigma-Aldrich,202142-100G) dissolved in water/IPA (1:1/v:v) in air, directly on the TiO_2 compact layer at 2500 rpm for 60 s, and then annealing for 30 min at 150 ^{o}C in air.

Perovskite solar cell fabrication: To form the perovskite layer, the non-stoichiometric precursor solution was made by mixing MAI (Dyesol) with $PbCl_2$ (Sigma-Aldrich, 268690-250G) at molar ratio of 3:1 in DMF at 35 wt%, which was spin-coated from a room temperature solution on the substrate at room temperature in a nitrogen-filled glovebox at 2000 rpm for 45 s. After spin-coating, the films were left to dry at room temperature in the glovebox for 60 minutes, to allow slow solvent evaporation prior to any annealing. This drying process is likely to be part responsible for the highly continuous films. They were then annealed on a hotplate in the glovebox at 90 °C for 150 min followed by 120 °C for 15 min. A hole-transporting layer was then deposited via spin-coating a 0.08 M solution of 2,2′,7,7′-tetrakis-(N,N-di-p-methoxyphenylamine)9,9′-spirobifluorene (spiro-OMeTAD) in chlorobenzene, with additives of 30 mol% lithium bis(trifluoromethanesulfonyl)imide and 80 mol% 4-tert-butylpyridine. Spin-coating was carried out at 2000 rpm for 45 s. Devices were then left overnight in dry box. Finally, 50 nm gold or 120 nm silver electrodes were thermally evaporated under vacuum of $\approx 10^{-6}$ Torr, at a rate of ≈ 0.2 nm·s^{-1}, to complete the devices.

Materials Characterization: The AFM images were taken with a SPA-400, Seiko. The UPS spectra were tested with ESCALab250Xi. The color-displaying experiment was performed by dipping the TiO_2/CsBr layer in the diluted $AgNO_3$/DMF solution. After a few seconds, the AgBr will form through reaction (1) and replace CsBr on the cp-TiO_2 layer. The unreacted $AgNO_3$ and by-products were removed by washing with deionized water. AgBr was then to strong UV light, which decomposed into Ag through reaction (2). A microscope was used to study the morphology of CsBr modified TiO_2 substrate.

$$CsBr(s) + AgNO_3(aq) \rightarrow AgBr(s) + CsNO_3(aq) \tag{1}$$

$$AgBr(s) + hv \rightarrow Ag(s) + Br_2(g) \tag{2}$$

The photocatalytic activity of TiO_2 without and with CsBr modification was evaluated by measuring the decomposition of methylene blue at 650 nm upon photoexcitation with a UV lamp (wavelength=365 nm, intensity=358 mW cm^{-2}). We employed mesoporous TiO_2 film herein rather than the compact TiO_2 since we required a large surface area of interaction between the TiO_2 and the methyl blue solution, in order to enable the measurement to be performed within a practical time. A 2 micron thick mesoporous TiO_2 layer was made by screen-printing of TiO_2 paste (dyesol 18NR-T), which was then sintered at 500 °C for 30 min. A CsBr solution of 2.5 mg/ml dissolved in water/IPA (1:1/v:v) was then spincoated on the TiO_2 compact layer at 2500 rpm for 30 s, and then annealing at 150 ^{o}C for 30 min in air. The mesoporous TiO_2 without and with CsBr modification was then immeresed in a methyl blue solution of 8 mg/L dissolved in anhydrous ethanol. The absorption intensity of the methyl blue solution was measured on a Varian Cary 300 (Agilent Technologies) every 1 h up to 6 h.

The X-ray diffraction (XRD) spectra were obtained via using a Panalytical X'Pert Pro x-ray diffractometer. A field emission scanning electron microscope (Hitachi S-4300) was used to acquire SEM images. Sample thicknesses were measured using a Veeco Dektak 150 surface profilometer. The UV-Vis absorbance of the perovskite films on TiO_2 blocking layer-coated FTO glass slides were measured on a Varian Cary 300 (Agilent Technologies). To reduce the sample variance, at least three samples were measured for each group and the average of all spectra presented. PL spectra were acquired using a time-resolved single photon-counting set-up (FluoTime 300, PicoQuant GmbH). Samples were photo-excited using a 507-nm laser head (LDH-P-C-510, PicoQuantGmbH) with pulse duration of 128 ps, fluence of 0.03 $\mu J \cdot cm^{-2}$ per pulse and a repetition rate of 300 KHz and 30 MHz. The UV irradiation was provided by UV resource (PORTA-RAY 400R). X-ray photoelectron spectroscopy (XPS) was obtained with a PHI 5300 ESCA Perkin-Elmer spectrometer. Mott-Schottky plots for devices with and without CsBr modification were measured at a frequency (*f*) of 10 kHz at a temperature (*T*) of 300 K.

Solar Cell Characterization: The current density–voltage (J-V) curves were measured with a 2400 Series SourceMeter (Keithley Instruments) under simulated AM 1.5 sunlight at an equivalent to 100 $mW \cdot cm^{-2}$ irradiance generated by an Abet Class AAB Sun 2000 simulator, with the intensity calibrated with an NREL calibrated KG5 filtered Si reference cell. The mismatch factor was calculated to be less than 1%. The solar cells were masked with a metal aperture to define the active area, typically 0.0919 cm^2 (measured individually for each mask) and measured in a light-tight sample holder to minimize any edge effects and ensure that the reference cell and test cell are located during measurement in the same spot under the solar simulator.

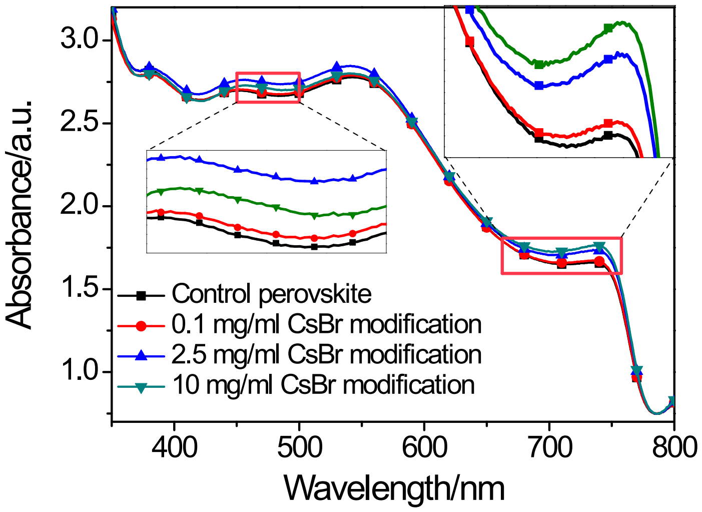

Figure S1 UV-Vis absorption spectra of $MAPbI_{3-x}Cl_x$ perovskite films coated upon FTO/c-TiO_2 substrates modified with CsBr cast from solutions of different concentrations.

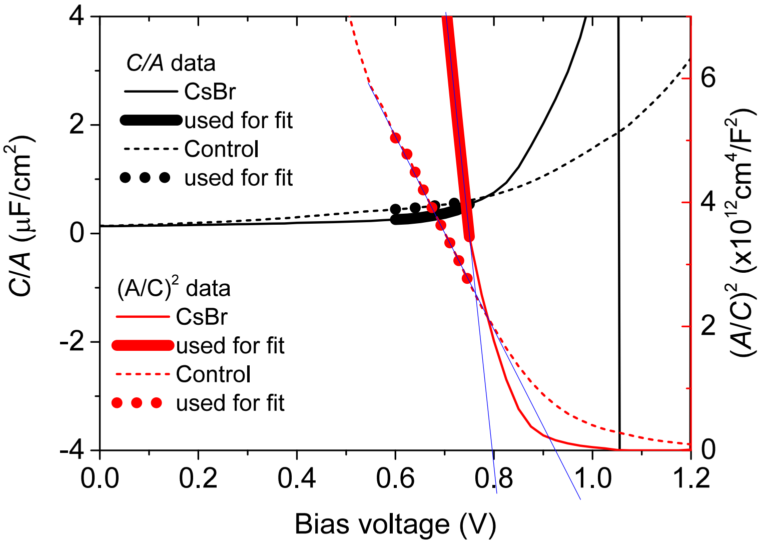

Figure S2 Mott-Schottky plots for devices with and without (control) CsBr modification were measured at a frequency (f) of 10 kHz at a temperature (T) of 300 K, where A is the area of the measured pixel. The blue lines are extrapolations to determine the built-in voltage.

Mott-Schottky plots are shown in Figure S2. From extrapolating the $(A/C)^2$ graphs to $(A/C)^2 = 0$ follows the built-in voltage (V_{bi}) (see table). The slope of the extrapolation can be used to determine the doping density N_d and the depletion width W (see table) at $V_{bias} = 0$ V:

$$N_d = - \frac{2}{q\varepsilon}\left(\frac{d(C/A)^{-2}}{dV}\right)^{-1}, \qquad (3)$$

$$w = \sqrt{\frac{2\varepsilon(V_{bi} - V_{bias})}{qN_d}}, \qquad (4)$$

where ε is the dielectric constant[1] (ε_r for this perovskite is 30)

	V_{bi} (V)	N_d (cm^{-3})	W (cm)
Device with CsBr	0.791	$5.92 \cdot 10^{16}$	$21.0 \cdot 10^{-6}$
Device without CsBr	0.925	$3.16 \cdot 10^{17}$	$9.8 \cdot 10^{-6}$

Temperature dependence of the frequency dependent capacitance is shown in Figure S3a and b for both types of cells. Steps are observed in these spectra that shift to lower frequency for lower temperature. The transition frequency can be related to the rate of carrier emission and capture from traps in the bandgap.[1] We assume that the occupancy of these states is in thermal equilibrium and hence is determined by the Fermi-Dirac distribution. Therefore the trap energy E_a and the characteristic transition frequency ω_0 can be expressed as:

$$\omega_0 = 2CT^2 exp\left(-\frac{E_a}{kT}\right), \qquad (5)$$

Where C is a constant related to the effective density of states in the conduction band, the thermal velocity and the carrier capture cross-section.[2] Now the activation energy can be determined from the plots in Figure S3c and d and Eq.(5). The activation energy of the traps was found to be roughly 0.23 eV for cells with and without CsBr.

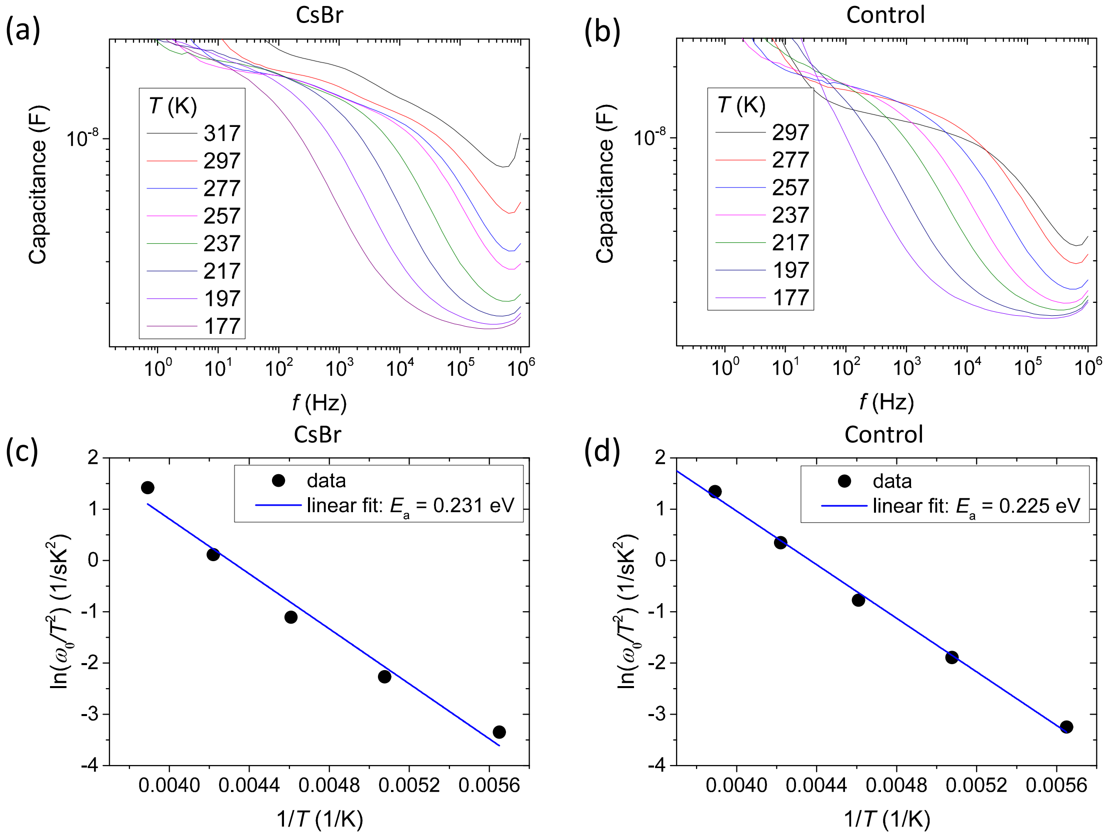

Figure S3 Temperature dependence of capacitance for (a) device with CsBr and (b) control device without CsBr. Arrhenius plot of the characteristic frequencies to extract the defect activation energy for (c) device with CsBr and (d) control device without CsBr.

Now the frequency dependent capacitance can be used to determine the energetic profile of the tDOS:

$$N_t = \frac{V_{bi}\, dC\, \omega}{qWd\omega kT}. \qquad (6)$$

The x-axis can be converted from frequency to energy by Eq. (5). The result is shown in the main text of this manuscript in Figure 3d.

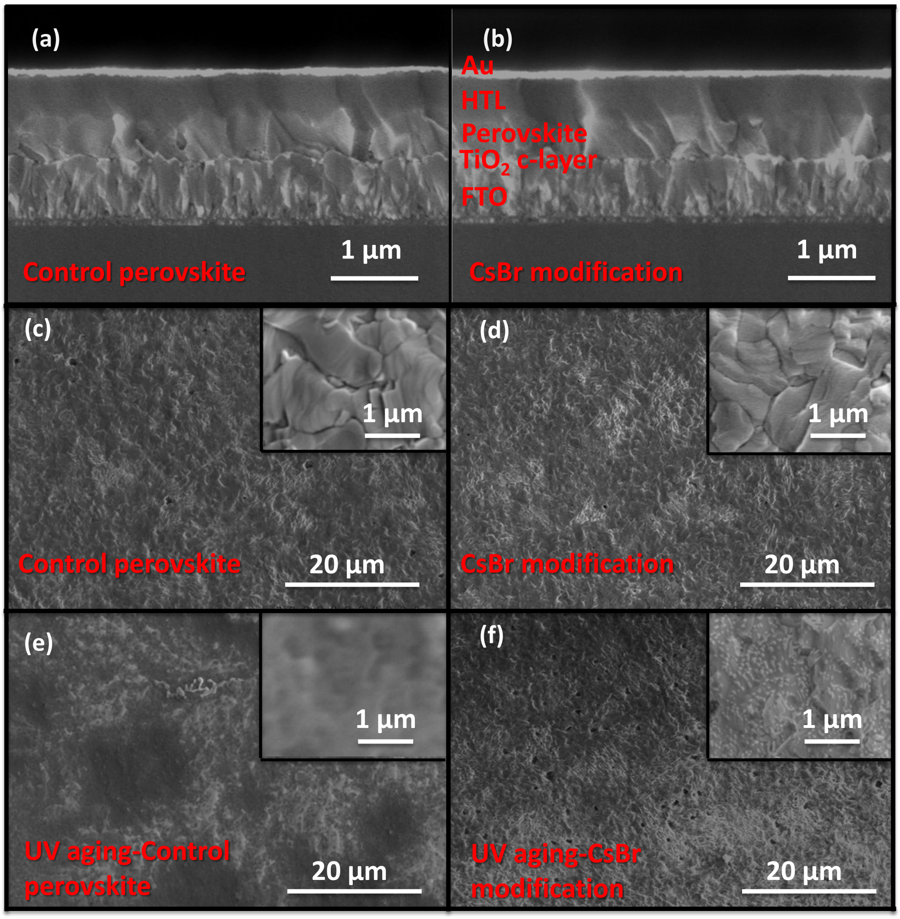

Figure S4 Cross-sectional SEM images showing device architecture of the planar heterojunction solar cells with (a) FTO/c-TiO_2/$CH_3NH_3PbI_3$/HTL/Au and (b) FTO/ c-TiO_2/CsBr/$CH_3NH_3PbI_3$/HTL/Au; SEM images of the top surfaces of (c) FTO/ c-TiO_2/$CH_3NH_3PbI_3$ and (d) FTO/c-TiO_2/CsBr/$CH_3NH_3PbI_3$ films before UV aging, (e) FTO/c-TiO_2/$CH_3NH_3PbI_3$ and (f) FTO/c-TiO_2/CsBr/$CH_3NH_3PbI_3$ films after UV aging of 100 min.

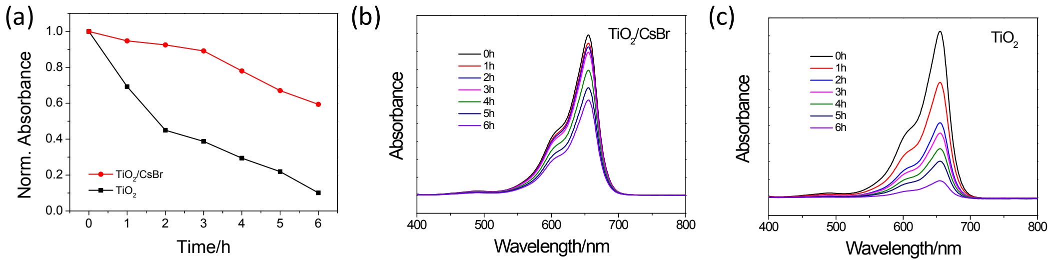

Figure S5 (a) Normalized absorbance of methyl blue in ethanol catalyzed by TiO_2 without (black curve) and with CsBr (red curve) modification, under different UV light (wavelength=365nm, intensity=364 mW cm^{-2}) soaking time. Absorbance of methyl blue in ethanol catalyzed by TiO_2 substrates with (b) and without CsBr (c) modification under diffierent UV light soaking time.

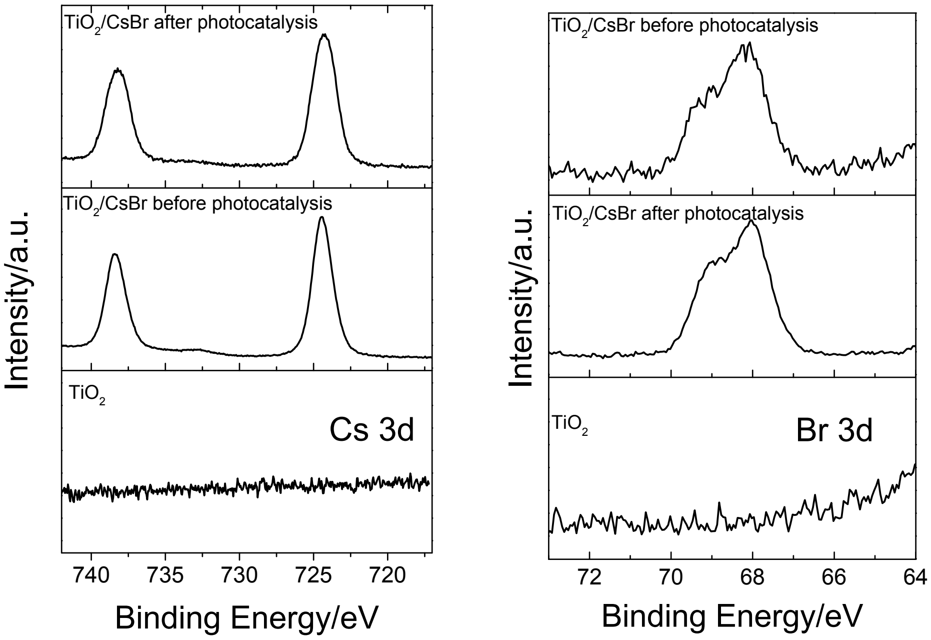

Figure S6 XPS spectra of $CsBr/TiO_2$ substrate before and after photocatalytic experiment.

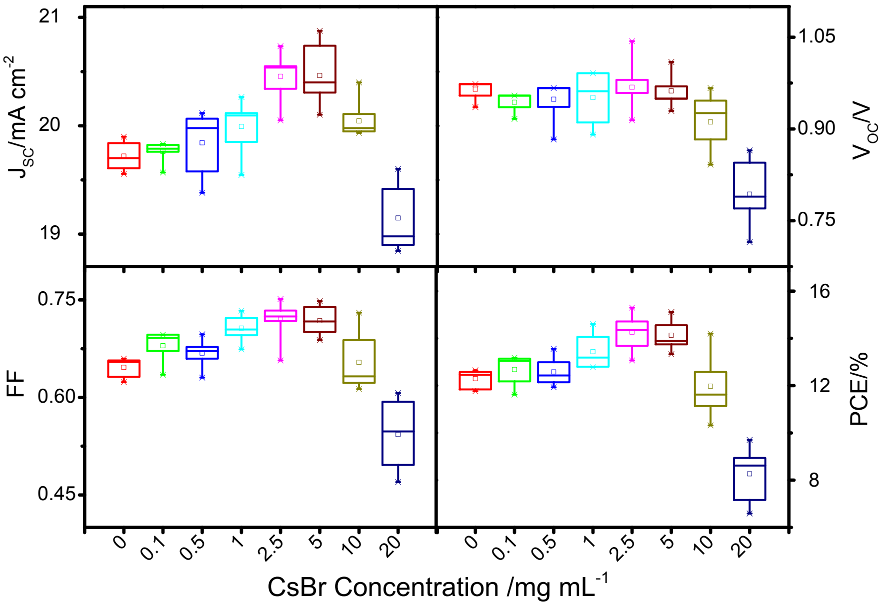

Figure S7 Device performance parameters with different CsBr concentration measured under simulated AM 1.5 sunlight of 100 mWcm^{-2} irradiance.

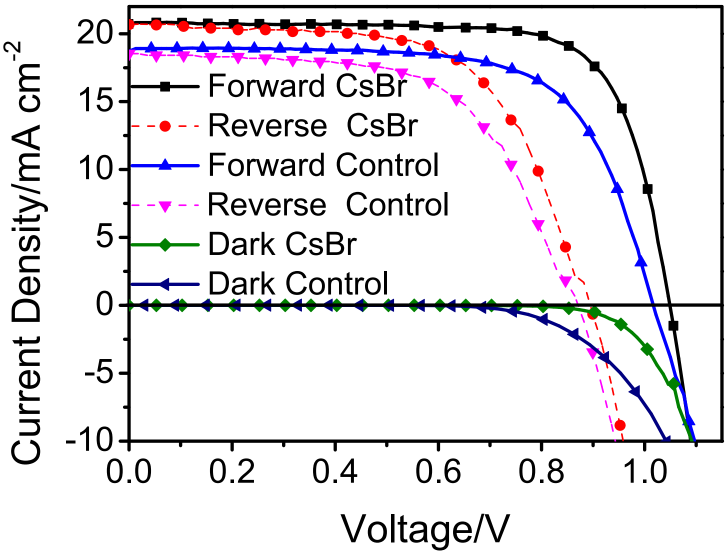

Figure S8 J–V curves of the best-performing device with and without CsBr modification measured under simulated AM 1.5 sunlight of 100 mW cm^{-2} irradiance and in the dark. The forward J–V scans were from forward bias to short circuit and the backward scans were from short circuit to forward bias, both at a scan rate of 0.15 V s^{-1}.

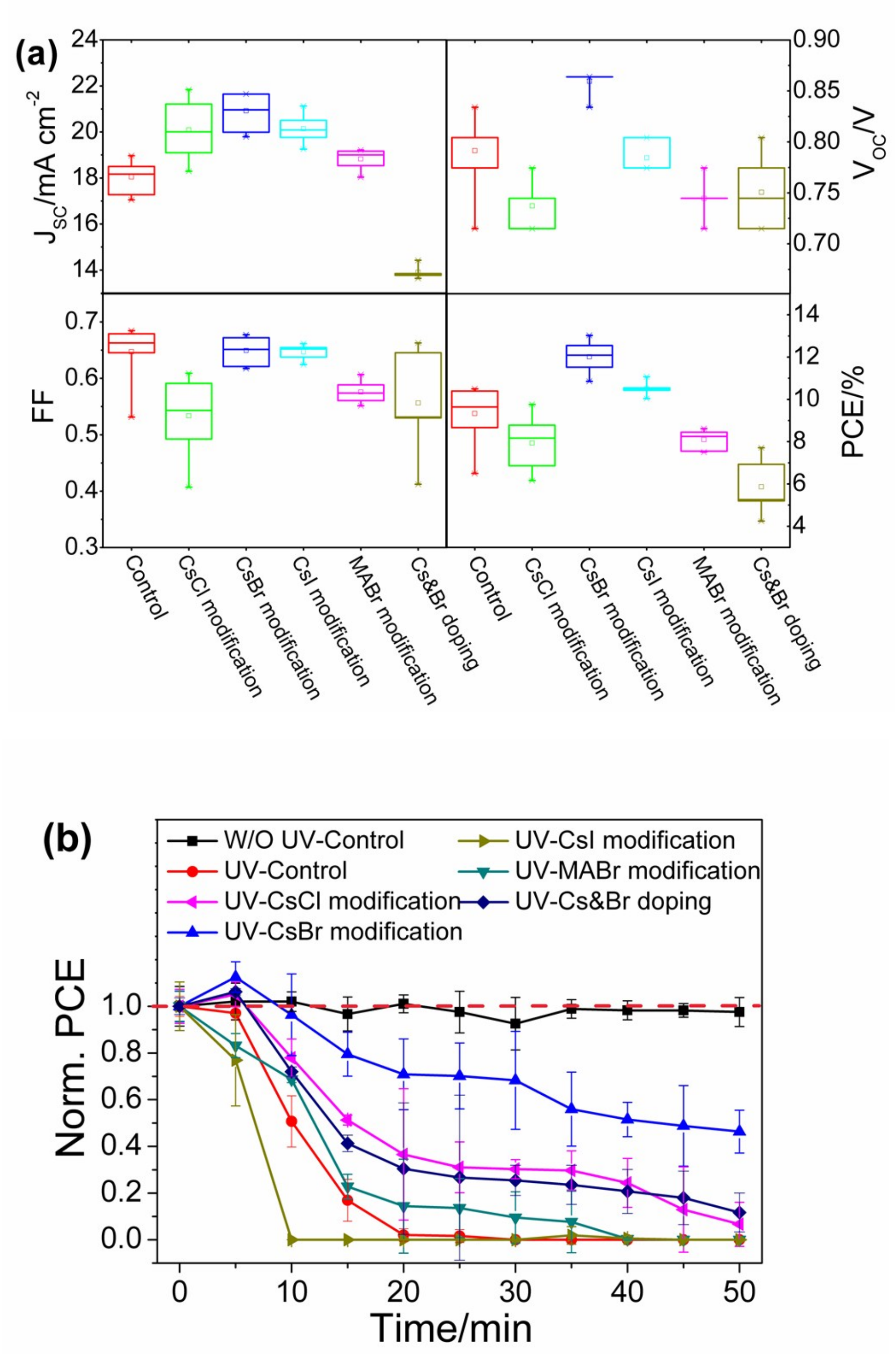

Figure S9 (a) Device performance parameters (at optimized concentration) with different interfacial modifiers (CsCl, CsBr, CsI, MABr) as well as the mixture solution of 5% CsI and 5% MABr for Cs and Br doping, measured under simulated AM 1.5 sunlight of 100 mWcm^{-2} irradiance. (b) Normalized device efficiency upon 50 min UV irradiation.

Table S1 Fitting parameters for the time-resolved PL measurements shown in Figure 3.

Samples	A_1	τ_1/ns	A_2	τ_2/ns	Average τ/ns
Glass/Perovskite	0.79	5.0	0.37	118.0	41.0
Glass/CsBr/Perovskite	0.38	20.8	0.52	177.6	111.4
c-TiO_2/Perovskite	0.23	1.66	1.17	18.9	16.0
c-TiO_2/CsBr/Perovskite	0.50	1.20	0.83	14.7	9.6

The PL decay can be fitted by a biexponential function:
$I(t)= A_1 \exp(-t/\tau_1) + A_2 \exp(-t/\tau_2) + y0$

where τ_1 (τ_2) represents the decay time of fast (slow) decay; A_1 (A_2) represents the amplitude of the fast-decay (slow-decay) component.

References

1. H. Duan , H. Zhou , Q. Chen , P. Sun , S. Luo , T. Song , B. Bob and Y. Yang, *Phys. Chem. Chem. Phys*. 2015,**17**, 112-116.
2. V. Gonzalez-Pedro, E. J. Juarez-Perez, W.-S. Arsyad, E. M. Barea, F. Fabregat-Santiago, I. Mora-Sero and J. Bisquert, *Nano Lett.*, 2014, **14**, 888–893.